Available Online at http://www.recentscientific.com

ISSN: 0976-3031

International Journal of Recent Scientific Research
Vol. 8, Issue, 3, pp. 15834-15838, March, 2017

International Journal of Recent Scientific Research

DOI: 10.24327/IJRSR

Research Article

CISS SEQUENCE AN AMELIORATOR OF MRI IN INTRACRANIAL PATHOLOGIES

Ramya Konareddy., Jeevika MU., Hari kiran Reddy R., Priyanka., Balaji Baliram Kale and Guru murthy B

Department of Radio Diagnosis, JJMMC, Davanagere

DOI: http://dx.doi.org/10.24327/ijrsr.2017.0803.0014

ARTICLE INFO

Article History:

Received 18th December, 2016
Received in revised form 10th January, 2017
Accepted 06th February, 2017
Published online 28th March, 2017

Key Words:

CISS, Cranial Nerves, Schwannoma, Intraventricular Web, CSF Cleft, Tumor

ABSTRACT

3D constructive interference in steady state (CISS) is a type of gradient echo MR sequence with accentuated T2 signal and increased T2/T1 contrast. CISS sequence is known for its use in cranial nerve visualisation and its pathologies but it is also of use in certain other pathologies as visualisation of scolex in NCC, intraventricular web visualisation, tumor delineation and CSF cleft visualisation. In this article we review the physics of CISS sequence and its advantages in the evaluation of various pathologies with few representative cases

INTRODUCTION

3D constructive interference in steady state (CISS) is a type of gradient echo MR sequence with accentuated T2 signal and increased T2/T1 contrast. This sequence is freely available and can provide accentuated information which is difficult to visualize with other sequences. It is known for its use in the cranial nerve visualization. Apart from this, it can also be used to better characterize a lesion when it is surrounded by CSF or fluid. Thus it is useful in evaluating ventricular pathologies, cystic lesions and delineation of tumors and identifying csf cleft in extra axial tumors.

Physics: Constructive interference in steady state (CISS) sequence is a type of slower version of fully refocused steady-state sequence with a shorter TR of approximately 15-20msec. In a CISS sequence two runs of SSFP sequence are done. In the first run a positive and negative flip angle is used and in the second run a constant flip angle is used. These two runs show mutually shifted banding artifacts which are then combined to eliminate the artifacts and obtain a CISS image.[1] CISS have many advantages over other steady state sequences. It has a shorter acquisition time owing to its short TR and TE. Tissues with long T2 relaxation like fluids will demonstrate wider ranges and additional signals owing to various refocused echo paths. It has a high signal-to-noise ratio and better contrast-to-noise ratio. It is insensitive to susceptibility, flow or motion related artifacts. CISS has different names according to different manufacturers: it is called fast imaging employing steady-state acquisition (FIESTA) by General Electric, true fast imaging with steady-state precession (FISP) by Siemens, balanced fast field echo (FFE) by Philips, and true steady-state free precession (SSFP) by Toshiba. CISS is mainly used in the assessment of the central nervous system, but it is also used when imaging the abdomen, the musculoskeletal system and the breast.[2]

Image characteristics: The image contrast of a particular tissue in CISS sequence depends on the inherent characteristic of the tissue in turn by the T2/T1 ratio of the tissue. Tissue with a long T2 and short T1 show high signal on CISS and appear as hyperintense. Such tissues are water and fat. Since the cerebro-spinal fluid (CSF) mainly consists of water we get a very high signal from it. Any structures which are surrounded by CSF show a striking difference in signal and hence are easily detected. Rest of the brain parenchyma has poor contrast and hence the grey-white differentiation in brain is poor.[3]

Clinical applications: As described above the ciss sequence plays a crucial role in evaluating structures surrounded by water /CSF. Specific applications are described below

**Corresponding author: Ramya Konareddy*
Department of Radio Diagnosis, JJMMC, Davanagere

Cranial nerve evaluation: CISS sequence is extremely useful in the detection of cranial nerves. Cranial nerves are thin structures arising from the brain, crossing across the cisterns and exiting from the skull foramina. As these nerves pass through the cisterns, they are surrounded by CSF and this results in high contrast difference which makes it possible to identify the nerves easily.

CISS sequence is useful in evaluating neurovascular conflict Certain arteries have been proposed to be consistently associated with the vascular conflict of certain nerves. Superior cerebellar artery is the most common artery associated with NVC of Vth nerve. In a few instances the anterior inferior cerebellar artery has also be seen to cause NVC with the Vth nerve.[4] Anterior inferior cerebellar artery was the most common artery in the NVC involving the VIIth and VIIIth nerves.[5]

Dolichoectasia of the vertebrobasilar system is due to uncertain pathogenesis. It is elongation and dilatation of vertebral and basilar arteries. In order to be classified as dolichoectasia in vertebrobasilar system, the basilar arterial diameter should be more than 4.5 mm.[6] The ectatic artery can impinge on the REZ of the cranial nerves. Since most of the cranial nerves emerge on the ventral aspect of the brain stem and the vertebra basilar artery are also located ventral to brain stem there is high possibility of them causing neurovascular conflict.[7] the dolichoctasia and its effect on the nerves can be appreciated best in CISS sequence. In a patient, referred to our department for MRI with clinical features of left trigeminal neuralgia, dolichoectasia of basilar artery causing neurovascular conflict was better appreciated in CISS sequence as seen in the fig 1

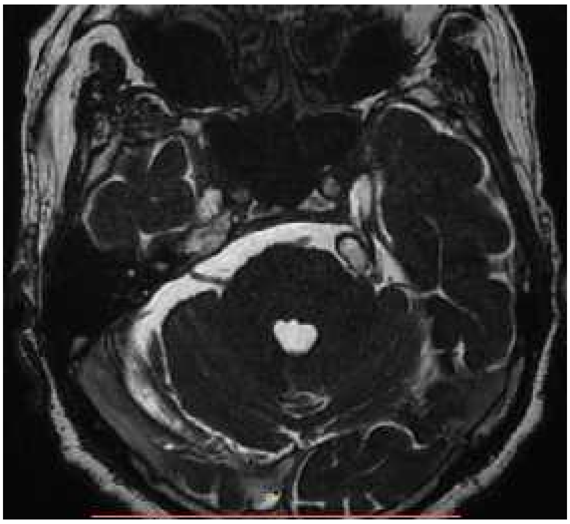

Fig1 Axial CISS image showing dolichoectasia of basilar artery causing neurovascular conflict of the left trigeminal nerve

The transition zone between the central (oligodendroglial) and peripheral (Schwann cell) portions of the eighth (vestibulocochlear) nerve, the presumed site of the origin of schwannomas of this nerve, occurs within the internal auditory canal. Tumors <5 mm in diameter can be reliably identified on CISS images, appearing as homogeneously mildly hypo- or iso-intense (to adjacent brain) ovoid or tubular intracanalicular mass, hypointense on T1WI with intense homogeneous contrast-enhancement. On T2W sequences, they appear mildly to markedly hyperintense and may be obscured by the similarity in signal intensity to that of the surrounding cerebrospinal fluid (CSF).[8]

Fundus of the internal acoustic meatus is its lateral end, the wall of which is formed by the thin cribriform plate of bone separating the cochlea and vestibule from the internal acoustic meatus; a transverse crest divides the fundus into two regions; in the superior region are located the facial nerve area and the superior vestibular area; in the inferior region are located the cochlear area, inferior vestibular area.[9] In case of CP angle tumours the involvement of fundus is important as it is directly related to the post operative complication of facial palsy.[10] Also extension into the inner ear has poor outcome post surgery. The extent of tumor extension into IAC can be better seen in CISS images as seen in fig2

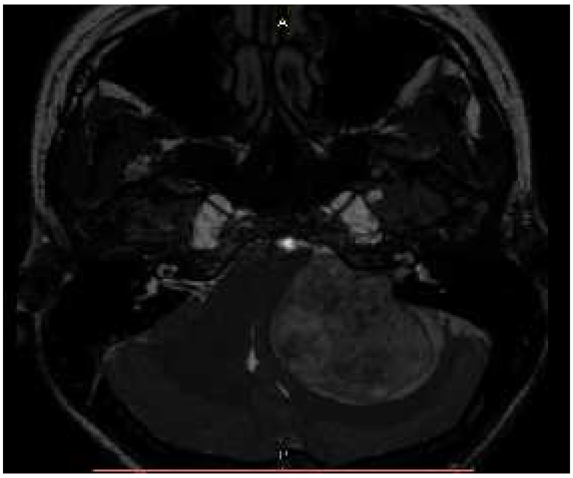

Fig 2a

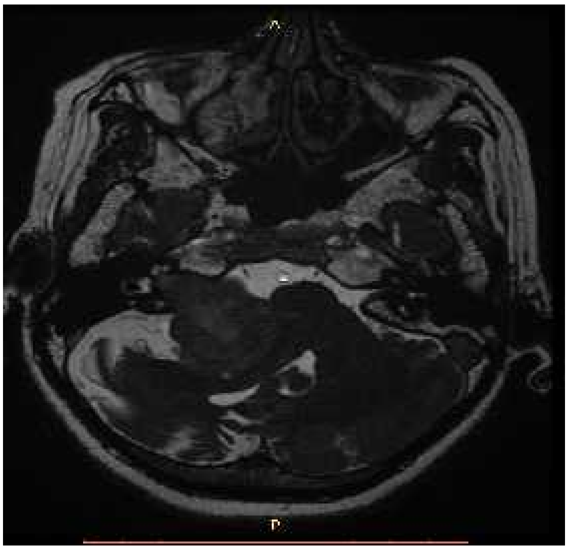

Fig2b

Fig 2 CP angle schwannoma in two different patient fig 2a showing tumor extension into iac but not reaching the fundus and fig 2b showing the tumor reaching the fundus of IAC

Trigeminal schwannomas are rare accounting for 0.07–0.3% of all intracranial tumours and 0.8%–5% of intracranial schwannomas.[11]The Meckel's cave houses the Gasserian ganglion and then gives off three branches: ophthalmic (V1), maxillary (V2) and mandibular (V3). In addition to conventional MRI sequences, CISS sequence should be obtained in patients with clinical suspicion of a trigeminal nerve lesion for better evaluation of the cisternal segment of the nerve.[12]

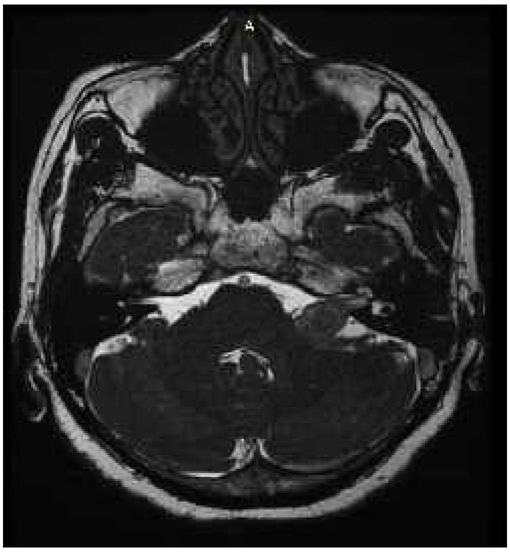

Fig 3 Axial CISS image showing left CP angle schwannoma, facial nerve can be clearly demarcated from the tumor there by giving the diagnosis of vestibular schwannoma

Cavernous sinus involvement is a contraindication for complete resection of a tumour. Findings which indicate invasion include compression, invasion or irregularity of the internal carotid artery (ICA) and loss of contrast enhancement of the cavernous sinus. Also another feature is the bulging of sinus wall which is usually concave.[13]

Intraventricular lesion evaluation: CISS sequence has a very high sensitivity in intraventricular lesions. The wall of small cysts can be easily made out. The relation of the tumour and extension through the foramen of lushka or Magendie in case of any tumour can also be easily demonstrated. Presence of thin intraventricular webs are visualized only in CISS as opposed to conventional sequences due to the thin slice thickness. Aqueduct stenosis and any fibrous adhesions are also better demonstrated.[14,15,16] The visualisation of web by ciss can be seen in fig 4

Fig 4 Sagittal ciss image showing intra ventricular web in a case of supraventricular hydrocephalus

Neurocysticercosis evaluation: It plays a role in the detection and characterization of small cysts in the brain especially neuricercous cysts. Cysts in neurocysticercosis have small eccentric scolex which can be missed on conventional sequences however CISS picks up these scolexes because of the high signal from water and low signal from scolex there is significant contrast difference. [17] The scolex appreciation by CISS can be seen in the fig 5

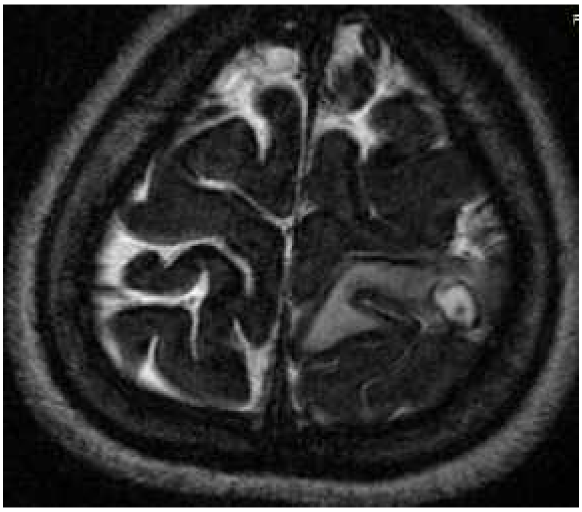

Fig 5 Neurocysticercosis in a 18 yrs old female with scolex and adjacent edema

Tumor evaluation: The visualization of a CSF cleft on CISS sequence allows for the differentiation between intra- and extra-axial tumors as appreciated in fig. The direction of displacement of the adjacent nerves and vessels gives a clue as to the location of the tumor. Intra-axial tumors will displace these laterally. The exact location and extent of the tumor and the presence of intra-tumoral cysts are also well visualized on this sequence. Tumors located in the subarachnoid space are better depicted on this sequence than on other sequences.[18,3] Thus helping the surgeons by exact plane of the tumor and its extension as seenin the fig 6

Fig 6 Axial CISS image in a case of sphenoidal meningioma showing csf cleft between the tumor and the brain parenchyma

CSF rhinorrhea: CSF rhinorrhea is condition where there is leakage of CSF into the paranasal sinuses and presence of fistula between the subarachnoid space and sinonasal cavity. It occurs most commonly following trauma. In such patients detection of leak is difficult with conventional MR sequences. The fistula is easily demonstrated using CISS owing to its thin slice thickness and the inherent high signal of the CSF. The depiction of continuous hyperintense CSF signal towards the extracranial area confirms the presence of leak and a defect resulting in CSF rhinorrhea. Even though CSF cisternography is superior to MR imaging the lack of ionizing radiation and non invasive procedure makes MR imaging the first choice for investigation for CSF rhinorrhea.[19]

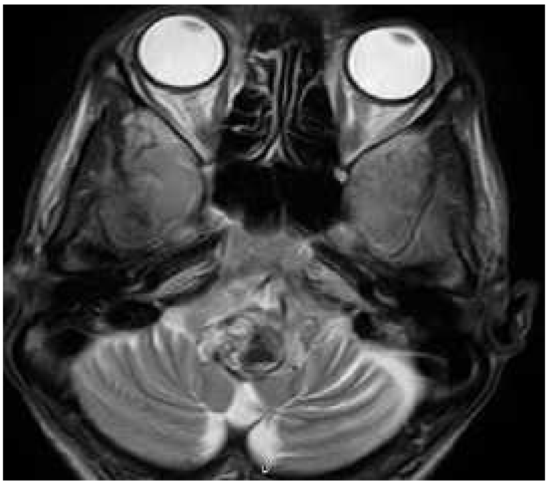

Fig7a

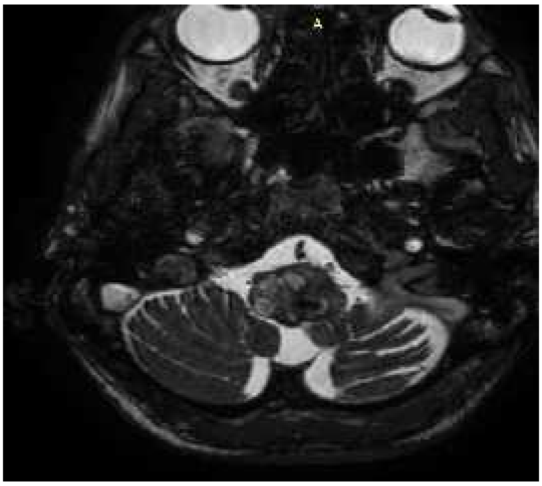

Fig7b

Fig 7 In a case of multiple granulomas in the brain, borders of the granuloma in the medulla were not well delineated T2 sequence(7a), which were better delineated in ciss sequence(7b)

Giant arachnoid granulations vs dural venous sinus thrombosis: It has certain benefit in differentiation of giant arachnoid granulations from dural venous sinus thrombosis. Arachnoid granulations are anatomical variants where the CSF space protrudes into the dural sinuses and these can be easily mistaken form pathology if especially large in size. These arachnoid granulations have CSF signal intensity on all imaging sequences. However the definite communication with the arachnoid space and defect in the duramater can only be demonstrated by CISS sequence and hence rules out possibility of any other pathology at that site.[20,21,3]

References

1. Chavhan GB, Babyn PS, Jankharia BG, Cheng H-LM, Shroff MM. Steady-state MR imaging sequences: physics, classification, and clinical applications. *Radiographics*. 2008;28(4):1147–60.
2. Gonçalves FG, do Amaral LLF. Constructive interference in steady state imaging in the central nervous system. *Eur Neurol Rev*. 2011;6(2):138–42.
3. Hingwala D, Chatterjee S, Kesavadas C, Thomas B, Kapilamoorthy TR. Applications of 3D CISS sequence for problem solving in neuroimaging. *Indian J Radiol Imaging*. 2011;21(2):90–7.
4. Lutz J, Linn J, Mehrkens JH, Thon N, Stahl R, Seelos K, *et al*. Trigeminal neuralgia due to neurovascular compression: high-spatial-resolution diffusion-tensor imaging reveals microstructural neural changes. *Radiology*. 2011; 258(2):524–30.
5. Gultekin S, Celik H, Akpek S, Oner Y, Gumus T, Tokgoz N. Vascular loops at the cerebellopontine angle: Is there a correlation with tinnitus? *Am J Neuroradiol*. 2008;29(9):1746–9.
6. Vieco PT, III EEM, Gross CE. Vertebrobasilar Dolichoectasia : Evaluation with CT Angiography. 1997;1385–8.
7. Campos WK, Guasti AA, da Silva BF, Guasti JA. Trigeminal Neuralgia due to Vertebrobasilar Dolichoectasia. *Case Rep Neurol Med*. 2012;2012:1–3.
8. Yadav P, Jantre M, Thakkar D. Magnetic resonance imaging of cerebellopontine angle lesions. *Med J DY PatilUniv* 2015; 8:751-9.
9. Salzman KL, Davidson HC, Harnsberger HR, Glastonbury CM, Wiggins RH, Ellul S, *et al*. Dumbbell schwannomas of the internal auditory canal. *Am J Neuroradiol*. 2001;22(7):1368–76.
10. Kocaoglu M, Bulakbasi N, Ucoz T, Ustunsoz B, Pabuscu Y, Tayfun C, *et al*. Comparison of contrast-enhanced T1-weighted and 3D constructive interference in steady state images for predicting outcome after hearing-preservation surgery for vestibular schwannoma. *Neuroradiology*. 2003;45(7):476–81.
11. Arseni C, Dumitrescu L, Constantinescu A. Neurinomas of the trigeminal nerve. *Surg Neurol*. 1975 Dec; 4(6):497–503.
12. Agarwal A. Intracranial Trigeminal Schwannoma. *Neuroradiol J*. 2015 Feb; 28(1): 36–41.
13. Raut A a, Naphade PS, Chawla A. Imaging of skull base: Pictorial essay. *Indian J Radiol Imagin*. 2012;22(4):305–16.
14. Yang D, Korogi Y, Ushio Y, Takahashi M. Increased conspicuity of intraventricular lesions revealed by three-dimensional constructive interference in steady state sequences. *Am J Neuroradiol*. 2000;21(6):1070–2.
15. Giuseppe Cinalli, W.J. Maixner CS-R. Pediatric Hydrocephalus. Springer Science & Business Media; 2012 Sep 10. 461 p.
16. Dinçer A, Kohan S, Özek MM. Is all “communicating” hydrocephalus really communicating? Prospective study on the value of 3D-constructive interference in steady state sequence at 3T. *Am J Neuroradiol*. 2009;30(10):1898–906.
17. Govindappa SS, Narayanan JP, Krishnamoorthy VM, Shastry CHS, Balasubramaniam A, Krishna SS. Improved detection of intraventricular cysticercal cysts with the use of three-dimensional constructive interference in steady state MR sequences. *Am J Neuroradiol*. 2000;21(4):679–84.
18. Ikushima I, Korogi Y, Hirai T, Sugahara T, Shigematsu Y, Komohara Y, *et al*. MR of Epidermoids with a Variety of Pulse Sequences. *Am J Neuroradiol*. 1997;18:1359–63.

19. Algin O, Hakyemez B, Gokalp G, Ozcan T, Korfali E, Parlak M. The contribution of 3D-CISS and contrast-enhanced MR cisternography in detecting cerebrospinal fluid leak in patients with rhinorrhoea. *Br J Radiol*. 2010 Mar;83(987):225–32.
20. Leach JL, Meyer K, Jones B V., Tomsick T a. Large arachnoid granulations involving the dorsal superior sagittal sinus: Findings on MR imaging and MR venography. *Am J Neuroradiol*. 2008;29(7):1335–9.
21. Leach JL, Jones B V., Tomsick T a., Stewart C a., Balko MG. Normal appearance of arachnoid granulations on contrast-enhanced CT and MR of the brain: Differentiation from dural sinus disease. *Am J Neuroradiol*. 1996;17(8):1523–32.

****

How to cite this article:

Ramya Konareddy *et al*. 2017, CISS Sequence An Ameliorator of Mri In Intracranial Pathologies. *Int J Recent Sci Res.* 8(3), pp. 15834-15838.